buildings

MDPI

Article

Optimal Determining Air Supply Humidity for Multi-Location Demands Under Different Objectives in an Indoor Moisture Environment: A Comprehensive Method and Case Study

Xiaojun Ma [1], Shuchen Yu [1], Xiaoliang Shao [2] and Jiujiu Chen [1,*]

[1] College of Biochemical Engineering, Beijing Union University, Beijing 100023, China; maxiaojun@buu.edu.cn (X.M.); 20232085910401@buu.edu.cn (S.Y.)
[2] School of Civil and Resource Engineering, University of Science and Technology Beijing, Beijing 100083, China; shaoxl@ustb.edu.cn
* Correspondence: chenjiujiu@buu.edu.cn

Abstract: Within high-precision indoor environments, such as semiconductor fabrication or textile plants, humidity control is paramount for preserving product integrity and reducing energy expenditure. The non-uniform indoor air environment poses a significant challenge in achieving humidity regulation that meets the distinct requirements of various locations. Traditional feedback control mechanisms may lead to instability, overshooting, and oscillation in indoor parameters. This paper proposes a comprehensive method to address humidity assurance issues in high-precision indoor environments by establishing analytical expressions that link the demand parameters at different locations with air supply parameters. Using a case study, this paper examines several typical operational scenarios with diverse control objectives, including minimizing dehumidification energy consumption, minimizing air supply humidity adjustment values, and constraints on adjustable air supply inlets. This method enables rapid calculation of air supply humidity and regulation of humidity parameters at multiple locations within the indoor environment. It considers various locations, requirements, optimization targets, and precision, demonstrating that it can quickly determine the optimal air supply parameters based on the objective function. This method facilitates rapid adjustment and high-precision assurance of different humidity requirements at multiple locations, making it suitable for high-precision design and control of indoor humidity environments.

Keywords: differentiated multi-location humidity; non-uniform environment; control strategy; regulation optimization; adjustment efficiency

Citation: Ma, X.; Yu, S.; Shao, X.; Chen, J. Optimal Determining Air Supply Humidity for Multi-Location Demands Under Different Objectives in an Indoor Moisture Environment: A Comprehensive Method and Case Study. *Buildings* **2024**, *14*, 3326. https://doi.org/10.3390/buildings14103326

Academic Editor: Eusébio Z.E. Conceição

Received: 19 September 2024
Revised: 14 October 2024
Accepted: 18 October 2024
Published: 21 October 2024

1. Introduction

The level of humidity in a given indoor environment has a significant impact on the quality of the air and the health of the occupants. Furthermore, it also affects the durability and functionality of products in civil and industrial buildings, especially in high-precision industrial environments [1–5]. Therefore, humidity assurance and control are important issues in the provision and maintenance of moist indoor environments. Humidity control is required for the production environment of many products, such as electronic products, pharmaceuticals, food, wood, and metal products, and building design standards always include humidity requirements [6].

In practical applications, the indoor humidity parameters that need to be guaranteed are not unique and fixed. In actual production and operation, one workshop or space usually contains several scenarios according to different production processes that will switch between each other. During this process, the indoor moisture sources and parameters do not always maintain a consistent state. Meanwhile, the actual distribution of indoor air parameters, such as humidity, is non-uniform under ventilation and air conditioning

modes, including displacement ventilation, personalized ventilation [7], and even mixed ventilation [8] and air curtain systems [9,10].

On the other hand, in the actual operation of industrial plants, corresponding optimized parameters and strategies are formulated for different objectives and control scenarios. Conventional methods of indoor humidity design and control are based on the lumped parameter approach, which is unable to guarantee the requirements of a non-uniform indoor environment. In fact, it may even result in increased energy consumption and reduced operational efficiency [11].

For the design and control of indoor non-uniform environments, the Computational Fluid Dynamics (CFD) technique can be used to predict the effects of different design or control scenarios [12–14]. However, it is challenging to apply to the complex or large number of calculation cases because of the long computing owing to the iterative process. When there are a variety of combinations and constraints of air supply parameters, it requires massive traversal calculation to obtain the optimal solution, which is very inefficient.

The most common methods for controlling indoor air humidity rely on feedback strategies [15,16]. The guaranteed parameters of different positions in a single room or space are different. When traditional feedback control strategies attempt to achieve high-precision satisfaction of guaranteed parameters at different positions simultaneously, it often results in control overshoot caused by continuous repeated adjustments, and even oscillation [17,18]. Although some scholars have attempted to achieve feedforward control to some extent using numerical calculation methods [19,20], most of the current feedforward control methods still rely on the accuracy of the prediction model of disturbance and progress for environmental parameter changes [21–24]. In general, some repetitions in the adjustment processes and time consumption are acceptable for most simple environmental controls so that these adjustment processes can satisfy the control requirements. However, for the complex situation of multiple locations and requirements mentioned previously, this method is inefficient and takes a lot of time and energy to meet the adjustment requirements.

Since the target parameters cannot be determined quickly or even in advance, the implementation of the strategy for input parameter optimization strategy based on the traditional operation method is complicated. The input parameters can only be evaluated during or after the adjustment and then changed or optimized, which makes it impossible to select an optimized strategy among several possible adjustment options.

In order to quickly obtain the distribution of indoor air parameters, some scholars have studied the contribution of different boundary and initial conditions to the indoor humidity at any point and the corresponding contribution indices under the stable airflow field and have developed algorithms based on these indicators, which are used to quickly calculate the indoor humidity distribution [24–26]. However, when determining the optimized air supply parameters to meet the different requirements of multiple indoor locations, although the contribution indices and calculation algorithms can be applied to calculate faster than CFD, it still needs to calculate a large number of cases using the ergodic method, so the efficiency of the optimization design has not been significantly improved. Thus, it cannot be directly used to guarantee the high-precision humidity parameters of multiple indoor locations under different objective functions.

In previous research on passive contaminants, the authors of this paper established the relationship between air supply and indoor contaminant concentrations in different locations [27–29].

In an indoor air environment, the transportation of water vapor is similar to that of a passive contaminant [25]. Based on our previous research on passive contaminants, in this paper, a comprehensive method for optimizing indoor humidity is proposed and an analytical model of the number of guaranteed positions and supply units that can independently adjust the air supply parameters in the same space is obtained. Using a case study, the model for non-uniform moisture environment optimization is applied to four different actual scenarios, allowing humidity parameters to be guaranteed simultaneously at different positions simultaneously in one space. This method establishes the relationship

between the demand of multiple locations and the air supply parameters, which can greatly improve the calculation efficiency of finding the optimal solution and realize the rapid adjustment and high-precision guarantee of different humidity parameters in multiple locations.

2. Methodology

2.1. Analytical Expression of Indoor Humidity Distribution

For indoor passive contaminants, the transport equation is well known and is given by Equation (1)

$$\frac{\partial \rho C(\tau)}{\partial \tau} + \frac{\partial \rho C(\tau) U_j}{\partial x_j} = \frac{\partial}{\partial x_j}\left(\Gamma_{Ceff} \frac{\partial C(\tau)}{\partial x_j}\right) + S_C(\tau) \quad (1)$$

$C(\tau)$: the contaminant concentration at time τ, (kg/kg).
Γ_{Ceff}: the effective diffusion coefficient of the passive gaseous contaminant, m^2/s.
$S_C(\tau)$: the rate of production of species, kg/s.

The transport equation of contaminant dispersion in a steady flow field is linear, and the superposition theorem is applicable [27]. The reference indicates that for indoor air flow, the transport equation of the moisture is the same as that of the gas contaminant, so the linear superposition theorem can also be used to solve the transport equation of indoor moisture dispersion [25].

Similar to the dispersion of a passive contaminant, indoor humidity distribution is determined by boundary conditions, including the moisture source, humidity of the air supply, and initial distribution of humidity in the subsequent moment. In typical indoor environments with air conditioning when the boundary conditions alter, the distribution of indoor parameters will reach a steady state within a relatively short timeframe. Therefore, this paper will focus on the steady-state situation. In our previous research, we proposed an algebraic algorithm for expressing the relationship between the humidity at an arbitrary position and all influencing factors of steady state [25].

When the steady state is reached, the humidity distribution of indoor space will only be affected by air supply and sources, which include internal sources and boundaries, and the humidity at an arbitrary point p can be represented by

$$d^p = \sum_{n_S=1}^{N_S}\left[d^{n_S} a_S^{n_S,p}\right] + \sum_{n_C=1}^{N_C}\left[\frac{J^{n_C}}{Q} a_C^{n_C,p}\right] \quad (2)$$

d^p: the humidity at an arbitrary point p, (kg/kg).
d^{n_S}: the humidity of the air supply at the n_Sth inlet, kg/kg.
J^{n_C}: the moisture emission rate of the n_Cth source, kg/s.
Q: the total room air flow rate, kg/s.
$a_S^{n_S,p}$: the accessibility index of the n_Sth air supply inlet to point p.
$a_C^{n_C,p}$: the accessibility index of the n_Cth moisture source to point p.

The two accessibility indices, $a_S^{n_S,p}$ and $a_C^{n_C,p}$, are defined to describe the contributions of the air supply and moisture source, respectively [25], that are quantified indicators of the ability of each boundary condition to influence different local points. They can quantify how easily moisture is delivered to an arbitrary position from the air supply inlet and moisture source. The accessibility values can be obtained using field measurements or numerical simulation.

2.2. Matrix Equations for Fast Calculating the Compensative Humidities of Air Supplies When Moisture Sources Change

Based on the analytical expression of the distribution of indoor humidity, a set of matrix equations of determination of the humidity variation of the air supply is proposed.

When the indoor moisture sources change, it can be treated as a change in the emission rate of the moisture source from J^{n_C} to $J^{n_C,*}$, which can be expressed as

$$\Delta J^{n_C} = J^{n_C,*} - J^{n_C} \tag{3}$$

$J^{n_C,*}$: the new emission rate of the n_Cth moisture source, kg/s.

ΔJ^{n_C}: the change in the emission rate of the n_Cth moisture source, kg/s.

In most industrial plants, the primary sources of moisture are manufacturing equipment. The location and emission intensity under different production scenarios could be considered as given. In addition, the human body is also considered a potential factor in the increase in indoor humidity. In the working environment, the location of workers and the emission rate of moisture are known in principle. When the location of personnel changes, it can also be determined using the source identification technology as the characteristics of indoor moisture dispersion can be regarded as passive contaminant characteristics and the change in the moisture source can be obtained using source identification technique [30,31]. Therefore, the position and emission rate of moisture sources are assumed as known in this study. For simplification, it is also assumed that the change in the emission rate of the moisture source is completed instantaneously, or that it can be treated as being completed in multiple time steps.

When the moisture source changes, the indoor air humidity distribution is going to be changed accordingly. Setting the total number of control points is N_p, which are recorded sequentially as 1...n_p...N_p, the change in humidity can be described by

$$\Delta d^{n_p} = d^{n_p} - d_0^{n_p} \tag{4}$$

d_0^p is the setting value of the humidity of point p, kg/kg.

d^{n_p} is the humidity of point p, kg/kg.

Δd^{n_p} is the change in humidity at point p from the setting value, kg/kg.

When the humidity demand of the control point remains unchanged, the aim of the control is to adjust the humidity d^{n_p} of point n_p to the original value $d_0^{n_p}$, i.e., $\Delta d^{n_p} = 0$. Therefore, the humidity of the air supply must be changed. If there are N_S air supply inlets in total, which are recorded as 1...n_S...N_S, the humidity of the n_Sth air supply inlet will be changed from $d_S^{n_S}$ to $d_S^{n_S,*}$

$$\Delta d_S^{n_S} = d_S^{n_S,*} - d_S^{n_S} \tag{5}$$

$d_S^{n_S}$: the original humidity value of the n_Sth air supply inlet, kg/kg.

$d_S^{n_S,*}$: the adjusted humidity value of the n_Sth air supply inlet, kg/kg.

$\Delta d_S^{n_S}$: the change in humidity of the n_Sth air supply inlet, kg/kg.

The objective of control is that there is a change in the emission rate ΔJ^{n_C} of moisture source n_C to recover the change in humidity of control point n_p to the setting value, which means $\Delta d^{n_p} = 0$ or an arbitrary constant value, and the adjustment for the air supply humidity $\Delta d_S^{n_S}$ of each air inlet n_S will be determined.

Considering that the indoor flow field is steady and that the walls are vapor-impermeable boundaries, there are a total of N_C moisture sources, N_S air supply inlets, and N_P humidity control points in the room.

According to Equation (2), when the emission rate of each moisture source changes and that change is ΔJ^{n_C}, if the air supply humidity does not change it is equivalent to superimposing an extra moisture source with an emission rate of ΔJ^{n_C} from the existing steady source. Thus, the humidity of control point n_P in the room at moment τ can be expressed as

$$d^{n_P} = \sum_{n_S=1}^{N_S} \left[d_S^{n_S} a_S^{n_S,n_P} \right] + \sum_{n_C=1}^{N_C} \left[\frac{J^{n_C}}{Q} a_C^{n_C,n_P} \right] + \sum_{n_C=1}^{N_C} \left[\frac{\Delta J^{n_C}}{Q} a_C^{n_C,n_P} \right]. \tag{6}$$

When the air supply humidity changes $\Delta d_S^{n_S}$ simultaneously, the humidity and change in control point n_P can be calculated as

$$d^{n_P} = \sum_{n_S=1}^{N_S} \left[d_S^{n_S} a_S^{n_S,n_P} \right] + \sum_{n_C=1}^{N_C} \left[\frac{J^{n_C}}{Q} a_C^{n_C,n_P} \right] + \sum_{n_S=1}^{N_S} \left[\Delta d_S^{n_S} a_S^{n_S,n_P} \right] + \sum_{n_C=1}^{N_C} \left[\frac{\Delta J^{n_C}}{Q} a_C^{n_C,n_P} \right], \quad (7)$$

$$\Delta d^{n_P} = \sum_{n_S=1}^{N_S} \left[\Delta d_S^{n_S} a_S^{n_S,n_P} \right] + \sum_{n_C=1}^{N_C} \left[\frac{\Delta J^{n_C}}{Q} a_C^{n_C,n_P} \right]. \quad (8)$$

In order to maintain operational state, it is necessary to restore the parameters of each control point to their original state, the average value of which is represented by $\Delta d^{n_p} = 0$. A set of matrix equations can be used to represent all N_P, as shown below.

$$\begin{bmatrix} \Delta d_S^1 \\ \vdots \\ \Delta d_S^{n_S} \\ \vdots \\ \Delta d_S^{N_S} \end{bmatrix} = -QS^{-1} \cdot C \begin{bmatrix} \Delta J^1 \\ \vdots \\ \Delta J^{n_C} \\ \vdots \\ \Delta J^{N_C} \end{bmatrix},$$

$$\mathrm{S} = \begin{bmatrix} a_S^{1,1} & \cdots & a_S^{n_S,1} & \cdots & a_S^{N_S,1} \\ \vdots & \ddots & & & \vdots \\ a_S^{1,n_P} & & a_S^{n_S,n_P} & & a_S^{N_S,n_P} \\ \vdots & & & \ddots & \vdots \\ a_S^{1,N_P} & \cdots & a_S^{n_S,N_P} & \cdots & a_S^{N_S,N_P} \end{bmatrix}. \quad (9)$$

$$\mathrm{C} = \begin{bmatrix} a_C^{1,1} & \cdots & a_C^{n_C,1} & \cdots & a_C^{N_C,1} \\ \vdots & \ddots & & & \vdots \\ a_C^{1,n_P} & & a_C^{n_C,n_P} & & a_C^{N_C,n_P} \\ \vdots & & & \ddots & \vdots \\ a_C^{1,N_P} & \cdots & a_C^{n_C,N_P} & \cdots & a_C^{N_C,N_P} \end{bmatrix}.$$

Considering the emission rate of each moisture source, ΔJ^{n_C} are known and C can be obtained in advance. By solving these equations, the adjustment of the air humidity $\Delta d_S^{n_S}$ of each air supply inlet can be calculated and the control target can be achieved.

There are N_P independent equations and N_S unknown variables in Equation (9); the solutions are listed below.

(1) $N_P = N_S$, the number of equations is equal to the number of unknown variables. Therefore, these equations have unique solutions. This indicates that there is a unique set of air supply humidity values to guarantee the humidity control requirements of all control points.

(2) $N_P \neq N_S$, S is transferred to a noninvertible matrix. When the $N_P < N_S$, the equations are indefinite; therefore, there are multiple solutions, which implies that there are multiple combinations of air supply humidity. Conversely, when $N_P > N_S$, the equations are over-determined; therefore, there is no solution, which implies that the control requirements of all control points cannot be guaranteed at the same time.

The above model shows that if $N_P \leq N_S$, the equations have at least one set of feasible solutions; thus, the target humidity of each control point can be achieved independently. Obviously, when the number of air supply inlets is not smaller than the number of control points, every control point can be guaranteed simultaneously. However, if $N_P > N_S$, the precise requirements of every control point will not be met simultaneously. Considering that the target parameters of some control points allow for a certain range of errors, it is possible to maintain the humidity of each control point within a certain range. In this case, the problem of solving the linear equations becomes a linear programming problem.

The preceding section outlines a rapid calculation method for obtaining air supply parameters. Once the parameters at the control points have reached a steady state, the aforementioned method can be employed to rapidly calculate the variables for each air supply parameter in the event of a change in operational procedure or moisture source. A schematic representation of the aforementioned method is presented in Figure 1.

The aforementioned method may be employed for the purpose of parameter optimization during the design phase, or alternatively, for real-time adjustment during the operational phase. It should be noted, however, that the actual operating scenarios are inherently complex, and as a result, a multitude of factors must be taken into consideration. These include the diversity of optimization objectives, the error range, economic impacts, predictable or unpredictable malfunction, and so forth. In instances where multiple factors are coupled, the process illustrated in the above figure is not applicable.

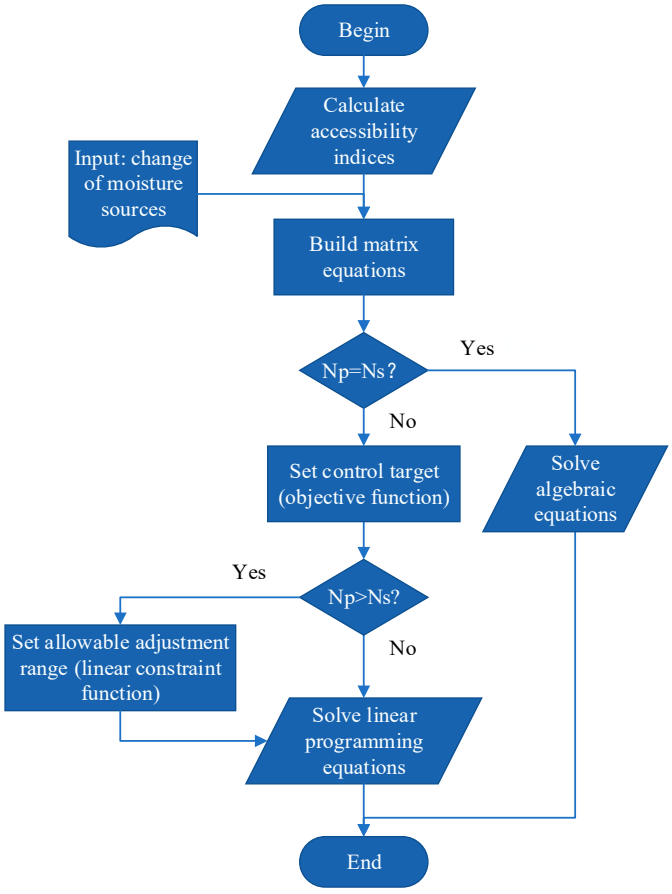

Figure 1. Schematic diagram of the quick calculation method for air supply parameters.

The following section will present a generalized scheme for the rapid optimization of air supply parameters from a control perspective, which will take into account a comprehensive range of operating conditions and objectives.

2.3. Optimal Regulation Strategy of Different Objective Functions

As previously discussed, when $N_P \geq N_S$, the equation has a unique solution or no solution. Consequently, it is impossible to compare and choose optimal air supply parameters for different objectives. If there exists an allowable adjustment range for control point n_P, which can be labeled as $\pm\delta d^{n_P}$, the linear constraint function can be expressed as

$$\text{s.t. } \Delta d_S^{n_S} - \delta d^{n_P} \leq \sum_{n_S=1}^{N_S} \left[\Delta d_S^{n_S} a_S^{n_S,n_P} \right] + \sum_{n_C=1}^{N_C} \left[\frac{\Delta J^{n_C}}{Q} a_C^{n_C,n_P} \right] \leq \Delta d_S^{n_S} + \delta d^{n_P}. \quad (10)$$

By establishing constraint functions in accordance with the permissible error range of control points, it becomes evident that there exists the potential for a multitude of solutions to the matrix equations. By defining distinct objective functions, the matrix equations can be transformed into a linear programming problem. There are various options for the objective function according to different regulation strategies. For example, for dehumidification conditions, the air supply control strategy has the minimum energy consumption as the target function to maximize the sum of the air supply humidity of each air supply inlet:

$$\max \sum_{n_S=1}^{N_S} d_S^{n_S,*}. \tag{11}$$

Alternatively, if the adjustability of each independent air supply is considered, the minimum parameter change in each air supply inlet is set as follows:

$$\min \sum_{n_S=1}^{N_S} \left|\Delta d_S^{n_S}\right|. \tag{12}$$

Similarly, when the other specific control objective function is considered, the optimization of the linear programming problem can be solved.

Therefore, by solving the equation above, the adjustment of the air supply humidity $\Delta d_S^{n_S}$ of each air supply inlet can be obtained.

In light of the actual operational scenarios, a comprehensive calculation method is proposed in order to guarantee the different parameter requirements at different positions. The diagrammatic representation of this method is provided below (Figure 2).

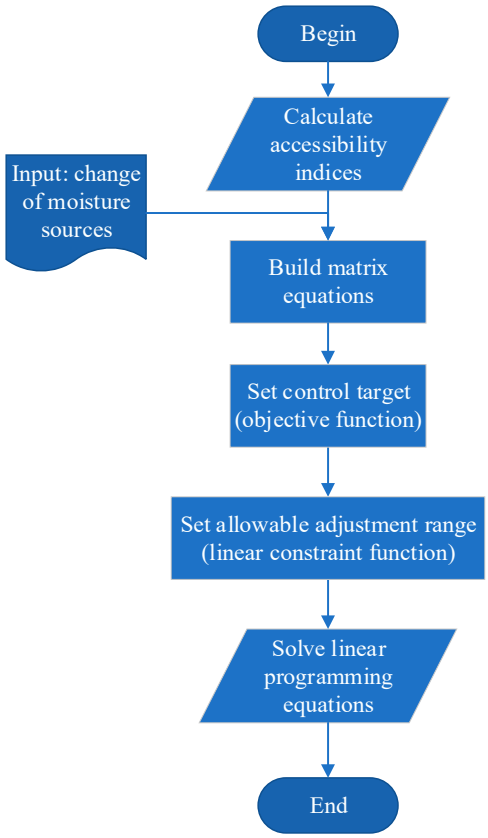

Figure 2. Schematic diagram of the comprehensive calculation method of the air supply parameters.

This method intuitively clarifies the control logic of the number of control points and number of adjustable air inlets and simply reveals the relationship between the changes in supplies and changes in needs. Thus, it can be applied to guarantee the control target and optimizes the control strategy.

3. Case Study: Parameter Optimization for Various Objectives

By the above method, the air supply parameters that need to be adjusted can be easily obtained when the control scene changes so as to quickly achieve the control goal and save the adjustment time. In this section, the application of the method for optimizing the parameters of air supply under different control objectives is presented using a case study.

3.1. Case Description

A geometric model of the ventilated room is shown in Figure 3. The room had dimensions of 13.6 m (L) × 3 m (H) × 6 m (W). The air conditioning was serviced by four fan coil units (FCUs), assuming the air supply parameter of each FCU could be adjusted independently. The four air supply inlets and four exhaust air outlets were labeled as S1 to S4 and R1 to R4, respectively, with dimensions of 0.3 m × 0.3 m (each). There were three pieces of equipment, as the moisture sources, labeled as C1 to C3, in the room; the emission rate of each source was 0.11 g/s. For simplicity, the moisture sources were treated as point sources. There were no other heat or contaminant sources in the room. The parameters for each air supply and moisture source are listed in Table 1. There were three control points, labeled as P1 to P3, in the room. The moisture sources and control points were in the same plane (Y = 1 m), as shown in Figure 4. The specific positions are listed in Table 2.

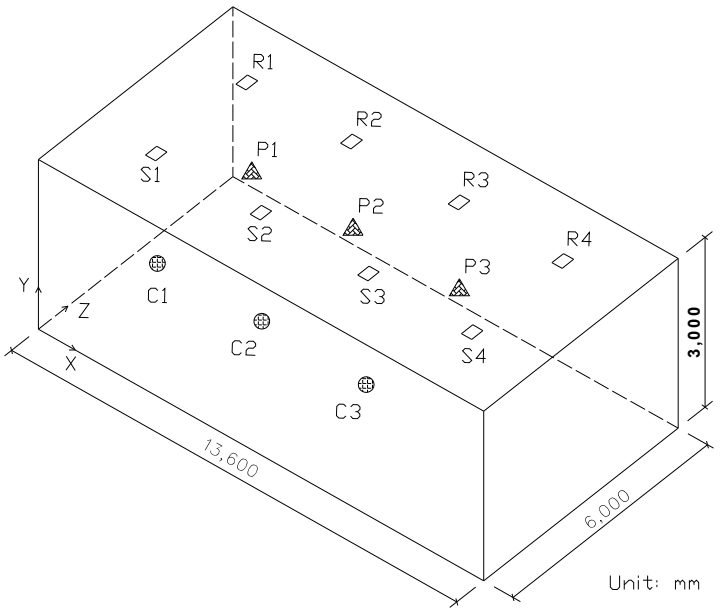

Figure 3. Geometric model of the ventilated room.

Table 1. Parameters of boundary conditions.

Air Supply/Moisture Source	Velocity (m/s)	Volume (kg/s)	Humidity (g/kg)	Emission Rate (g/s)
S1	1.0	0.108	9.85	—
S2	1.0	0.108	9.85	—
S3	1.0	0.108	9.85	—
S4	1.0	0.108	9.85	—
C1	—	—	—	0.11
C2	—	—	—	0.11
C3	—	—	—	0.11

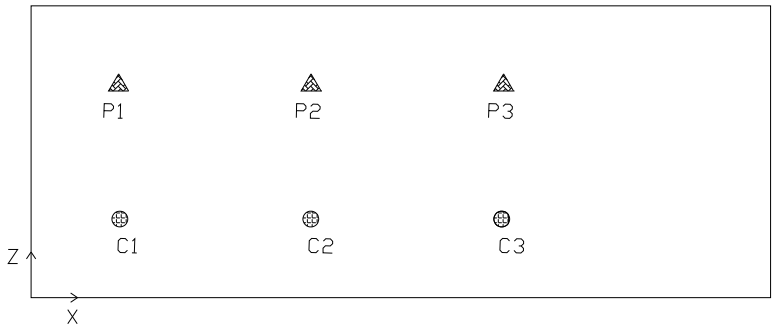

Figure 4. Location of moisture sources and control points (Y = 1 m).

Table 2. Positions of moisture sources and control points.

Point	X (m)	Y (m)	Z (m)
C1	1.7	1	1.5
C2	5.1	1	1.5
C3	8.5	1	1.5
P1	1.7	1	4.5
P2	5.1	1	4.5
P3	8.5	1	4.5

When the operation scenario switched, the humidity source C3 ceased operation, resulting in a rapid decline in the emission rate from 0.11 g/s to 0 g/s. The control target was to maintain the humidity of each control point at the steady state unchanged. The initial parameters of the case calculation are listed below (Table 3).

Table 3. Initial parameters of case calculation.

Source	ΔJ^{n_C} (g/s)	Control Point	Δd^{n_P} (g/kg)
C1	0	P1	0
C2	0	P2	0
C3	−0.11	P3	0

According to the calculation method proposed in this paper, in the first step, the accessibility of each air supply inlet and moisture source could be obtained by CFD simulation in advance, and then the changes in the humidity of each air supply inlets were calculated with different scenarios, respectively, in the following steps.

The computational fluid dynamic (CFD) software STACH-3 was used to determine the indoor flow field and accessibility indices. An indoor zero-equation turbulence model [14] was selected to account for turbulent flow indoors. The Reynolds-averaged Navier–Stokes (RANS) equations, together with the averaged energy and mass conservation equations, were discretized using the finite-volume method (FVM). The difference scheme was a power-law scheme. The SIMPLE algorithm was employed. Momentum equations were solved on non-uniform staggered grids [32]. The simulation tool was well validated by Zhao et al. [33].

CFD was used to calculate the flow field of the room in Figure 3 as well as the accessibility of the air supply and moisture sources. After the grid-independence study, the room was discretized by 20,250 structured hexahedral meshes.

3.2. Non-Uniform Airflow Filed and Accessibility

The simulated steady flow field is shown in Figure 5. The humidities of the control points were 10.83 g/kg for P1, 10.81 g/kg for P2, and 10.59 g/kg for P3.

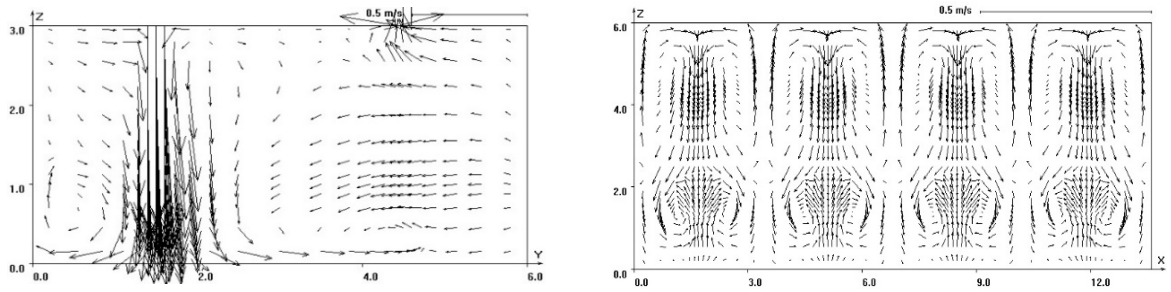

(**a**) X = 5.1 m (**b**) Y = 1 m

Figure 5. Distribution of the flow field at typical planes.

The accessibility values of each air supply inlet moisture source on the control points at the steady state are listed in Table 4.

Table 4. Accessibility of the air supply and moisture source on the control points at the steady state.

	S1	S2	S3	S4	C1	C2	C3
P1	0.73	0.20	0.06	0.01	2.82	0.91	0.11
P2	0.24	0.55	0.19	0.02	1.05	2.14	0.59
P3	0.02	0.19	0.55	0.24	0.17	0.59	2.14

In this case, the number of air inlets was greater than the number of control points. According to Equation (9), there were several air supply parameters that could meet the humidity requirements of the three control points. Four different scenarios were set for the solution to achieve different control strategies as listed in Table 5.

Table 5. Four different scenarios.

Scenario	Solution	Objective
I	$N_P < N_S$	Minimization of the dehumidify consumption
II	$N_P < N_S$	Minimization of the adjustment value of air supply humidity
III	$N_P = N_S$	Limitation of the adjustable air supply inlets: number of adjustable air inlets equal to control points
IV	$N_P > N_S$	Limitation of the adjustable air supply inlets: number of adjustable air inlets less than control points

3.3. Scenario I Minimization of the Dehumidify Consumption

According to the objective function in Equation (11), the air supply humidity of each inlet was calculated, as listed in Table 6. The minimal total increase in the air supply humidity of the air inlets was 1.56 g/kg.

Table 6. Humidity of the air supply for Scenario I.

	S1	S2	S3	S4
Original humidity (g/kg)	9.85	9.85	9.85	9.85
Adjusted humidity (g/kg)	9.82	9.92	10.40	10.82

Figure 6 shows the humidity distribution of the room at the steady state after the adjustment of the air supply parameters. The humidity at each control point remains unchanged compared with the original values.

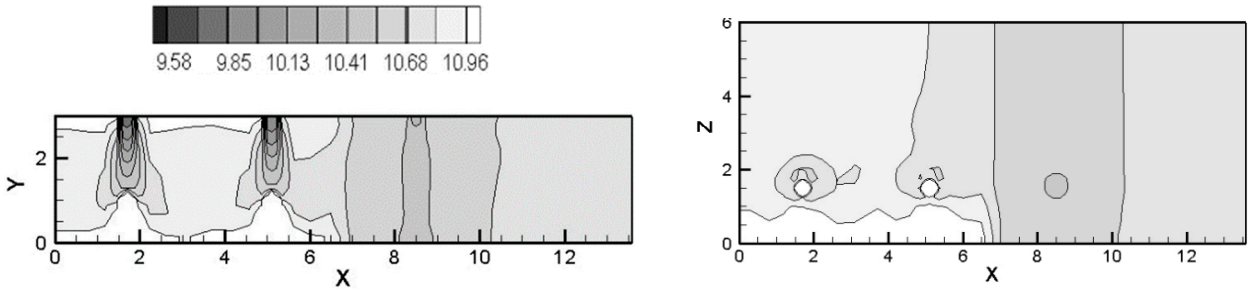

(**a**) Z = 1.5 m (**b**) Y = 1 m

Figure 6. Indoor humidity distribution after adjustment for Scenario I (g/kg).

3.4. Scenario II Minimization of the Adjustment Value of Air Supply Humidity

According to the objective function in Equation (12), the air humidity of each air supply inlet was calculated, as listed in Table 7. The sum of the humidity increments in the air supply inlets was 0.99 g/kg. Compared with Case 1, the value was lower, which indicated a higher energy consumption.

Table 7. Humidity of the air supply for Scenario II.

	S1	S2	S3	S4
Original humidity (g/kg)	9.85	9.85	9.85	9.85
Adjusted humidity (g/kg)	9.82	9.80	10.82	9.95

3.5. Scenario III Limitation of Adjustable Air Supply Inlets: Number of Adjustable Air Inlets Equal to Control Points

It was assumed that the air supply humidity at inlet S2 was not able to be adjusted; thus, the number of adjustable air inlets was equal to that of control points. According to Equation (9), the solution was unique, as listed in Table 8, and a precise control of each control point could be achieved. The sum of humidity increments in the air supply inlets was 1.24 g/kg. Compared with Scenario I and II, the value was between them, which also implied that the energy consumption was in the middle.

Table 8. Humidity of the air supply of Scenario III.

	S1	S2	S3	S4
Original humidity (g/kg)	9.85	9.85	9.85	9.85
Adjusted humidity (g/kg)	9.82	9.85	10.63	10.34

3.6. Scenario IV Limitation of Adjustable Air Supply Inlets: Number of Adjustable Air Inlets Less than Control Points

In the above three scenarios, the number of air inlets was larger than or equal to the number of control points. However, in some engineering projects, the number of air supply inlets whose supply parameters could be independent-adjusted was less than the positions that needed to be guaranteed. According to the previous analysis of this study, it is impossible to accurately guarantee every control point simultaneously unless the control point allows some error range.

In this scenario, the air supply inlet S4 was unable to adjust the humidity owing to some faults, and its air supply humidity was maintained at 9.85 g/kg. A new control point labeled as P4 was added, which was located on the same plane as the other control points; the specific position is listed in Table 9. In this scenario, the number of air inlets was three, while the number of control points was four.

Table 9. Position of control point P4.

Position	X (m)	Y (m)	Z (m)
P4	11.9	1	4.5

According to the above calculation, the humidity of P4 at the steady state was 10.11 g/kg. In this scenario, the control target parameters of P1 to P4 could not be met simultaneously and precisely by adjusting the humidity of the air supply inlets S1 to S3. Setting the allowable humidity range of each control point as ±0.2 g/kg, multiple sets of air supply humidities satisfying the control requirements could be obtained by solving the equations. Tables 10 and 11 list the results that correspond to the minimum energy consumption at the control target. The sum of humidity increments in the air supply inlets was 1.40 g/kg. Figure 7 shows the indoor humidity distribution after adjustment. The humidities of the various control points were within the allowable range.

Table 10. Humidity of the air supply for Scenario IV.

	S1	S2	S3	S4
Original humidity (g/kg)	9.85	9.85	9.85	9.85
Adjusted humidity (g/kg)	10.05	10.08	10.82	9.85

Table 11. Humidities of control points with the minimum energy consumption for Scenario IV.

	P1	P2	P3	P4
Target humidity (g/kg)	10.83	10.81	10.59	10.11
Actual humidity (g/kg)	10.95	10.94	10.75	10.29
Deviation (g/kg)	+0.12	+0.13	+0.14	+0.18

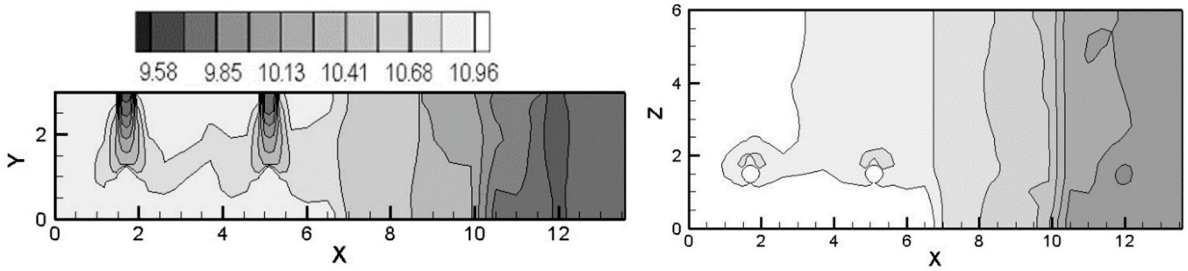

(**a**) Z = 4.5 m (**b**) Y = 1 m

Figure 7. Indoor humidity distribution after adjustment of Scenario IV (g/kg).

In addition, considering that there were multiple solutions in the accuracy range of this scenario, it was indicated that the humidity adjustment range of the control point could be further narrowed, thereby improving the control accuracy.

4. Discussion

The comprehensive method for indoor humidity control presented above was based on the calculation of indoor moisture distribution. The algebraic expression had been validated and demonstrated in previous work. Ma et al. verified the expression by comparing the predicted value with the experimental measurements of several points in a ventilated room. The data of the humidity predicted by the analytical expression agreed acceptably with the experimental measurements [25].

To reveal the availability of this method for indoor parameter control, a humidity adjustment process in an experimental room with traditional feedback control methods and the new method proposed in this paper were measured and compared. In order to provide

a clear demonstration of the characteristics of the adjustment process and to take into account the limitations of the measurement conditions, a single-control-point experiment was conducted for comparison.

The experimental platform was located at Beijing Union University, which included the test chamber and air conditioning system, as shown in Figure 8. The overall size of the test chamber was 6.5 m (L) × 2.5 m (H) × 4 m (W) and enclosed with foam-polyurethane material which could be treated as heat and moisture isolation. The air conditioning system of this experiment consisted of a system with complete air circulation (fresh air and exhaust air were both closed).

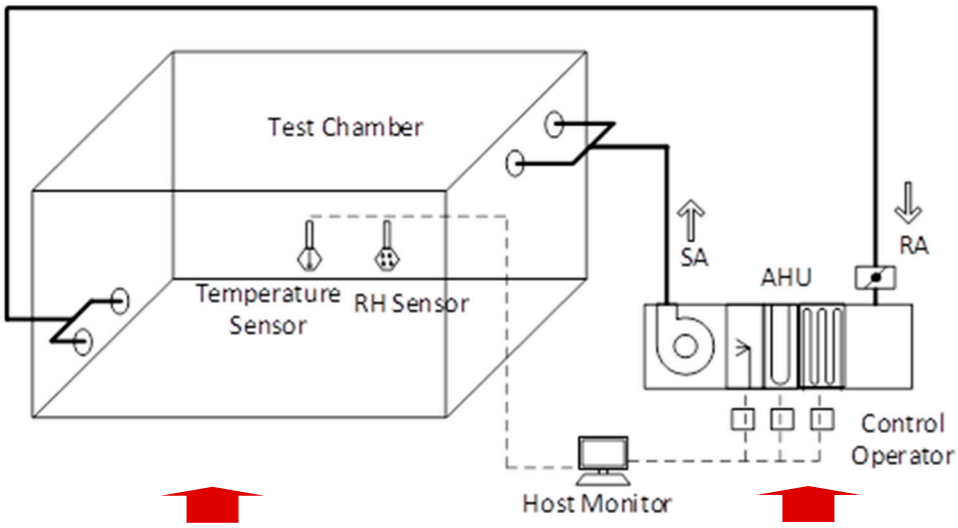

(**a**) Test chamber.

(**b**) AHU.

Figure 8. Indoor climate experimental platform.

The initial temperature of the experimental test chamber was 25 °C and the relative humidity was 40%. The supplied air volume was 940 m^3/h (~15 air exchanges) and the air speed of the inlet was 1.85 m/s. A calibrated ultrasonic humidifier with a strength of 700 g/h was utilized as the moisture source. One measurement point was arranged in the artificial climate chamber. Specific information of the test equipment is listed in Table 12 as well as the experimental setting in Table 13. The temperature and humidity were recorded every 10 s. The moisture source and control points were located on the symmetrical surface of the room, as shown in Figure 9.

Table 12. Specification parameters of the experimental equipment.

Instrument Name	Role	Measurement Range	Accuracy
RHLOG-T-H temperature and humidity self-reporter	Monitor indoor humidity	0~100% RH −30~+70 °C	±3% RH Indoor environment: ±0.5 °C Outdoor environment: ±1 °C
HMP110 ambient temperature and humidity sensor	Monitor indoor temperature and humidity	0~100% RH −40~+80 °C	± 1.5% RH −40~0 °C: ±0.4 °C 0~40 °C: ±0.2 °C 40~80 °C: ±0.4 °C

Table 13. The control setting of the experimental procedure.

Time (s)	0	150
Emission rate of moisture source (g/h)	700	0
Setting value of relative humidity (%RH)	40	40

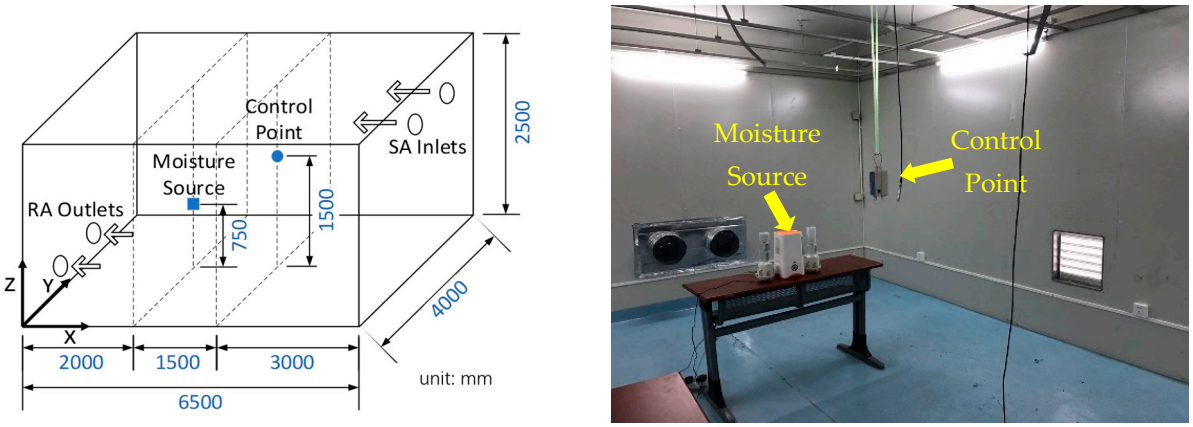

Figure 9. Location of the moisture source and control point.

Setting the moisture sources emission rate as 700 g/h at the beginning of measurement, the indoor humidity pattern remained relatively stable at a value of 40% RH. When the indoor moisture source suddenly stopped at 150 s, under the traditional feedback control strategy, the indoor humidity rapidly dropped, reaching a trough at a value of 33.1% RH, which is shown in Figure 10a. The control loop of the traditional method was needed to compare the indoor measured value with the set value, thereby explaining the long reaction time. At a time of 360 s, the feedback signal caused the humidifier to work so that the indoor humidity began to rise and approach the set value of 40% RH at 630 s. At 720 s, a steady state was achieved. Since the PID control algorithm was used in the control of the actuator, there was no overshooting during the process.

With the new control method, since the required air supply parameters could be quickly calculated according to the change in the humidity source, the humidifier could directly adjust the amount of humidification without sensor feedback. Figure 10b presents the experimental results and confidence interval of these two different control methods. It can be seen that when the humidity source suddenly disappeared, the indoor humidity began to drop, and the lowest humidity of 37.1% RH was achieved at 260 s. Then, the humidity value began to rise and achieved a steady state at 470 s.

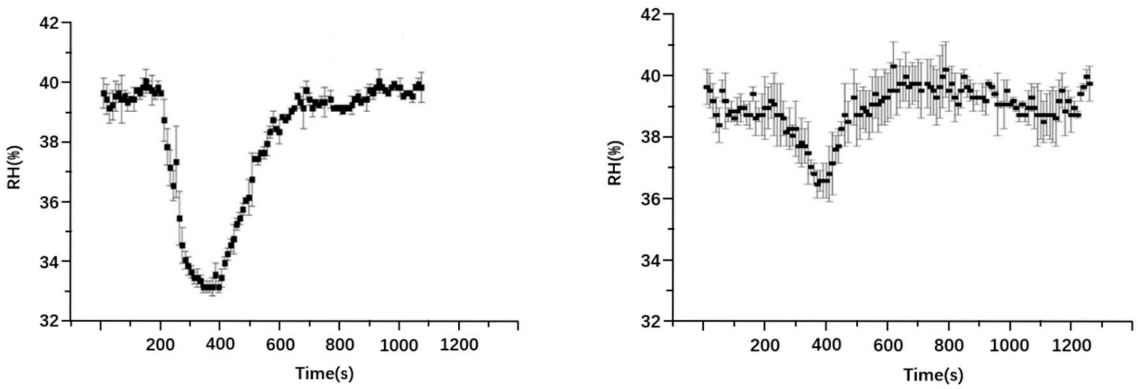

(**a**) Traditional feedback control method. (**b**) New control method.

Figure 10. Experimental results of two different control methods.

Comparing the humidity changes under the two adjustment processes, it can be seen that the humidity reduction in the traditional method took more time to reach the minimum, and the humidity reduction (6.9% RH) was greater than the reduction with the new method (2.9% RH). When the humidity was close to the set value (40% RH), the humidity of the new method control also approached the set value and rapidly achieved a steady state.

Also, Figure 10 indicates that the curve using the new method exhibited an obvious jump due to the great change in the humidity value compared with the previous moment, and the confidence interval was wider. Overall, from the analysis of the data error, the error of the result was within the allowable range and the experimental results are thus reliable.

The proposed optimization method can be used to rapidly determine the air supply parameters of each air outlet that meet different control objectives. The followed step-by-step implementation process was used as a guide for indoor moisture control in real projects:

Step 1: Calculate the accessibility indices of each air supply and moisture source based on the physical characteristics, manufacturing processes, and indoor airflow properties of the room.

Step 2: Input the change in moisture sources, which can either be pre-set according to different production scenarios or detected online during operation. Then, establish a matrix equation system and set the target function for regulation.

Step 3: Set the allowable adjustment range for the humidity values at each control point; it may be set to zero for precise control or to an appropriate value for loose control.

Step 4.1: Solve linear programming equations to obtain the variation of air supply parameters for each air supply outlet. This marks the conclusion of the calculation process and the generation of the output values.

Step 4.2: In the event that the variation of each air supply outlet is unable to meet the control requirements of each control point or the optimization goals of regulation, the allowable adjustment range of each control point must be reset and the process must be returned to Step 3.

5. Conclusions

Based on the algebraic expression of indoor air humidity distribution under steady flow field, a comprehensive optimization method for indoor non-uniform moisture environment control was developed in this study. With a case analysis, the method was applied to guarantee the indoor multi-location humidity with different objectives. The main conclusions of this paper are drawn as follows.

(1) This paper presents a comprehensive method for multi-location demands under different objectives in an indoor moisture environment with varying control error ranges. By rapidly calculating with a matrix equation, the variations of air supply parameters can be timely determined for different control scenarios. The matrix equations in this paper

reveal the relationship between the number of adjustable air supply inlets and the number of controllable locations. When the air supply humidity can be adjusted independently, the proposed method is used to determine the air supply humidity parameters to satisfy the requirements of each control point. The corresponding solutions may be optimized for different control objectives by setting the humidity adjustment range of control points within an allowable range.

(2) Using the case study, the application of the proposed method for indoor non-uniform moisture environment guarantee was illustrated. With different objective conditions, which include minimization of the dehumidify consumption, minimization of the adjustment value of air supply humidity, and limitation of adjustable air supply inlets, the strategies of the air supply parameters under different control targets were analyzed. Optimization of the control strategy according to different objective functions can be achieved using this method.

(3) Compared with traditional feedback regulation methods, the proposed method shows an advantage in adjusting indoor environment parameters. This study involved the establishment of an experimental setup for a typical regulation process in which two different control methods were used to measure the change in humidity. The results showed that the method proposed in this paper is more effective in the reaction and recovery time of the control system and the amplitude of deviation from the set value.

Based on the discussions of availability and feasibility of the proposed method, a step-by-step implementation process is drawn as the guideline for control optimization in real projects. The method can be applied for the control of indoor air humidity to meet different multi-location demands. It is of significant value for the adjustment and control of indoor environment in high-precision buildings.

Author Contributions: Conceptualization, X.M. and J.C.; methodology, X.M. and S.Y.; software, X.S.; validation, X.S. and S.Y.; formal analysis, J.C.; investigation, J.C. and S.Y.; resources, X.M.; data curation, X.S.; writing—original draft preparation, J.C. and X.S.; writing—review and editing, X.M. and S.Y.; visualization, S.Y. and X.S.; supervision, X.M.; project administration, X.M.; funding acquisition, X.M. and X.S. All authors have read and agreed to the published version of the manuscript.

Funding: This research was funded by the National Natural Science Foundation of China, grant number 51578065 and 51878043 and Research project on Beijing Risk Prevention Control Theory and Key Technologies Based on Big Data, grant number ZB102006.

Data Availability Statement: The original contributions presented in the study are included in the article, further inquiries can be directed to the corresponding author.

Conflicts of Interest: The authors declare no conflicts of interest.

References

1. Scislo, L.; Szczepanik-Scislo, N. Influence of mechanical ventilation and cooling systems on vibrations of high precision machines. *E3S Web Conf.* **2019**, *100*, 00080. [CrossRef]
2. Mendes, A.S.P.; Rutgersson, A.; Paulsson, M. Outdoor environmental effects on cleanrooms—A study from a Swedish hospital pharmacy compounding unit. *Eur. J. Pharm. Biopharm.* **2022**, *177*, 100–106. [CrossRef] [PubMed]
3. Milton, O.; James, R.L. *Reliability and Failure of Electronic Materials and Devices*, 2nd ed.; Academic Press, Inc.: Cambridge, MA, USA; 6277 Sea Harbor Drive Orlando: Orlando, FL, USA, 2009; pp. 56–78.
4. Purushothama, B. *Humidification and Ventilation Management in Textile Industry*, 1st ed.; CRC Press: London, UK, 2024; pp. 135–164.
5. Zou, Y.Y.; Clark, J.D.; May, A.A. A systematic investigation on the effects of temperature and relative humidity on the performance of eight low-cost particle sensors and devices. *J. Aerosol Sci.* **2021**, *152*, 7–10. [CrossRef]
6. Bellia, L.; Minichiello, F. A simple evaluator of building envelope moisture condensation according to an European standard. *Build. Environ.* **2003**, *38*, 457–468. [CrossRef]
7. Melikov, A.K.; Cermak, R.; Majer, M. Personalized ventilation: Evaluation of different air terminal devices. *Energy Build* **2002**, *34*, 829–836. [CrossRef]
8. Heiselberg, P. Room air and contaminant distribution in mixing ventilation. *ASHRAE Trans.* **1996**, *102*, 332–339.
9. Shen, C.; Shao, X.; Li, X. Potential of an air curtain system orientated to create non-uniform indoor thermal environment and save energy. *Indoor Built Environ.* **2017**, *26*, 152–165. [CrossRef]

10. Park, D.Y.; Chang, S. Numerical investigation of thermal comfort and transport of expiratory contaminants in a ventilated office with an air curtain system. *Indoor Built Environ.* **2019**, *28*, 401–421. [CrossRef]
11. Cai, H.; Li, X. Balancing Indoor Environment Quality and Energy Use with a Human-oriented Evaluation Method of Indoor Air Distribution. In Proceedings of the First International Conference on Building Energy and Environment (COBEE 2008), Dalian, China, 13–16 July 2008.
12. Jones, P.J.; Whittle, G.E. Computational fluid dynamics for building air flow prediction-current status and capabilities. *Build. Environ.* **1992**, *27*, 321–328. [CrossRef]
13. Nielsen, P.V. Numerical prediction of air distribution in rooms-status and potentials. In Proceedings of the Conference on Building Systems: Room Air and Air Contaminant Distribution, Urbana-Champaign, IL, USA, 5–8 December 1988.
14. Chen, Q.; Xu, W. A zero-equation turbulence model for indoor airflow simulation. *Energy Build.* **1998**, *28*, 137–144. [CrossRef]
15. Wang, Y.; Kuckelkorn, J.M.; Li, D.; Du, J. A novel coupling control with decision-maker and PID controller for minimizing heating energy consumption and ensuring indoor environmental quality. *J. Build. Phys.* **2019**, *43*, 22–45. [CrossRef]
16. Husein, H.; Budiman, M.; Djama, M. Duty Cycle Control on Compressor of Split Air Conditioners Using Internet of Things Embedded in Fuzzy-PID. *Int. J. Electr. Eng.* **2019**, *11*, 112–124. [CrossRef]
17. Underwood, C.P. *HVAC Control Systems: Modelling, Analysis and Design*; E & FN Spon: London, UK, 1999; pp. 198–238.
18. Sun, Y.; Zhang, Y.; Guo, D. Intelligent Distributed Temperature and Humidity Control Mechanism for Uniformity and Precision in the Indoor Environment. *IEEE Internet Things J.* **2022**, *9*, 19101–19115. [CrossRef]
19. Shnayder, D.A.; Abdullin, V.V.; Basalaev, A.A. Building heating feed-forward control based on indoor air temperature inverse dynamics model. In Proceedings of the World Congress on Engineering and Computer Science, San Francisco, CA, USA, 22–24 October 2014.
20. Thomas, B.; Soleimani-Mohseni, M.; Fahlén, P. Feed-forward in temperature control of buildings. *Energy Build.* **2005**, *37*, 755–761. [CrossRef]
21. Wang, H.; Chen, M. Trajectory tracking control for an indoor quadrotor UAV based on the disturbance observer. *Trans. Inst. Meas. Control* **2016**, *38*, 675–692. [CrossRef]
22. Dullinger, C.; Struckl, W.; Kozek, M. A general approach for mixed-integer predictive control of HVAC systems using MILP. *Appl. Therm. Eng.* **2018**, *128*, 1646–1659. [CrossRef]
23. Pang, X.; Duarte, C.; Haves, P.; Chuang, F. Testing and demonstration of model predictive control applied to a radiant slab cooling system in a building test facility. *Energy Build.* **2018**, *172*, 432–441. [CrossRef]
24. Lee, S.; Kim, M.J.; Pyo, S.H.; Kim, J.T.; Yoo, C.K. Evaluation of an optimal ventilation IAQ control strategy using control performance assessment and energy demand. *Energy Build.* **2015**, *98*, 134–143. [CrossRef]
25. Ma, X.; Li, X.; Shao, X.; Jiang, X. An algorithm to predict the transient moisture distribution for wall condensation under a steady flow field. *Build. Environ.* **2013**, *67*, 56–68. [CrossRef]
26. Huang, H.; Kato, S.; Hu, R.; Ishida, Y. Development of new indices to assess the contribution of moisture sources to indoor humidity and application to optimization design: Proposal of CRI(H) and a transient simulation for the prediction of indoor humidity. *Build. Environ.* **2011**, *46*, 1817–1826. [CrossRef]
27. Li, X.; Chen, J. Evolution of contaminant distribution at steady airflow field with an arbitrary initial condition in ventilated space. *Atmos. Environ.* **2008**, *42*, 6775–6784. [CrossRef]
28. Ma, X.; Shao, X.; Li, X.; Lin, Y. An analytical expression for transient distribution of passive contaminant under steady flow field. *Build. Environ.* **2012**, *52*, 98–106. [CrossRef]
29. Shao, X.; Li, X.; Ma, X.; Chen, C. Optimising the supply parameters oriented to multiple individual requirements in one common space. *Indoor Built Environ.* **2014**, *23*, 828–838. [CrossRef]
30. Zhang, T.; Chen, Q. Identification of contaminant sources in enclosed environments by inverse CFD modeling. *Indoor Air.* **2007**, *17*, 167–177. [CrossRef]
31. Li, X.; Zhao, B. Accessibility: A new concept to evaluate the ventilation performance in a finite period of time. *Indoor Built Environ.* **2004**, *13*, 287–293. [CrossRef]
32. Launder, B.E.; Spalding, D.B. The numerical computation of turbulent flows. *Comput. Method. Appl. M.* **1974**, *3*, 269–289. [CrossRef]
33. Zhao, B.; Li, X.; Yan, Q. A simplified system for indoor airflow simulation. *Build. Environ.* **2003**, *38*, 543–552. [CrossRef]